CARBON 86 (2015) 118–123

Available at www.sciencedirect.com

ScienceDirect

journal homepage: www.elsevier.com/locate/carbon

A tubing shaped, flexible thermal energy harvester based on a carbon nanotube sheet electrode

Hee Doo Yang [a], Lemma Teshome Tufa [b], Kyoung Min Bae [b], Tae June Kang [a,b,*]

[a] Department of NanoMechatronics Engineering, College of Nanoscience and Nanotechnology, Pusan National University, Busan 609-735, South Korea

[b] BK21 Plus Nano Convergence Technology Division, College of Nanoscience and Nanotechnology, Pusan National University, Busan 609-735, South Korea

ARTICLE INFO

Article history:
Received 17 October 2014
Accepted 16 January 2015
Available online 22 January 2015

ABSTRACT

A tubing-shaped, flexible electrochemical thermal energy harvester (thermocell), which can be wound around various types of waste heat sources, was fabricated. The thermocell utilizes the temperature dependence of the ferri/ferrocyanide ($Fe(CN)_6^{3-}/Fe(CN)_6^{4-}$) redox potential, providing a thermoelectric coefficient of ~1.4 mV/K. A highly porous carbon nanotube (CNT) sheet, which is wrapped onto a thin platinum (Pt) wire, was used as an electrode for the redox reaction. The electrode performance was examined by comparing the output powers from the thermocells using a bare Pt wire and CNT sheet wound electrodes. The CNT sheet electrode showed a higher output power from 8.5 to 15.6 μW, and the short-circuit current density (j_{sc}) was increased ~1.8 times compared to that of the Pt wire electrode. The performance of the CNT sheet based thermocell was examined according to the winding number of the CNT sheet, the temperature difference between the two electrodes and the operating temperature. The series connection of the thermocells, to demonstrate the voltage and power scaling, was also examined with an understanding of the primary internal resistance that limits the output electrical power.

1. Introduction

A tremendous amount of waste heat is released from everyday life, such as air-conditioning, vehicles, lighting, and home appliances. This waste heat is typical available at temperatures below 100 °C and released to surrounding environment. The use of a thermoelectric device is one of the possible ways of scavenging waste heat. Based on the Seebeck effect, a thermoelectric generator is capable of the direct conversion of temperature differences to an electrical voltage. In the past few decades, considerable efforts have been made to improve the conversion efficiency of thermoelectric generators [1–8]. However, the small thermoelectric coefficient (typically several tens to hundreds of microvolts per Kelvin) [9–12] remains an obstacle to the delivery a sufficient voltage and electric power, particularly when utilizing the temperature difference between the waste heat source and ambient environment. Inflexible and expensive thermoelectric materials have limited applicability to certain shapes of the heat source and large-area installations. Accordingly, researchers have focused on not only enhancing the thermoelectric performance, but also

* *Corresponding author at:* Department of NanoMechatronics Engineering, College of Nanoscience and Nanotechnology, Pusan National University, Busan 609-735, South Korea.
E-mail address: tjkang@pusan.ac.kr (T.J. Kang).
http://dx.doi.org/10.1016/j.carbon.2015.01.037
0008-6223/

on finding an alternative way to effectively harvest waste heat energy [13,14].

Liquid thermoelectric generators (*i.e.*, thermal electrochemical cells or thermocells) have recently attracted considerable attention in the thermal energy conversion [13,15–22]. A thermocell utilizes the temperature dependence of the redox potential of an electrolyte, which can provide a 10–100-fold higher thermoelectric coefficient (several millivolts per Kelvin) than those of conventional thermoelectric materials [13,23]. With the steady efforts in finding high-performance thermoelectric electrolyte and electrode materials, a low cost per watt of power conversion is envisioned as one of the major advantages of thermocell utilization. Using a flexible electrode and package materials to complete thermocell fabrication, the thermocell can be wrapped around the rounded heat sources without any degradation of performance.

In this study, a tubing-shaped, flexible electrochemical thermal energy harvester (thermocell), which can be wound around various types of waste heat sources, was fabricated. The thermocell utilizes temperature dependence of the ferri/ferrocyanide ($Fe(CN)_6^{3-}/Fe(CN)_6^{4-}$) redox potential, providing a thermoelectric coefficient of 1.4 mV/K. A highly porous carbon nanotube (CNT) sheet that is wrapped around a thin platinum (Pt) wire was used as an electrode for the redox reaction. The performance of the thermocell was investigated quantitatively according to the winding numbers of the CNT sheet, temperature difference between the two electrodes and operating temperature of the thermocell. To demonstrate the voltage and power scaling, the series connection was also examined with an understanding of the internal resistance that limits the output electrical power.

2. Experimental section

2.1. Operation principle of a thermocell

The thermoelectric potential in a thermocell is generated by the temperature dependence of the free energy difference between reactant and product of a reaction taking place at the electrolyte–electrode interface [13,20,23]. The operation of a thermocell is described schematically in Fig. 1(a). The CNT sheet electrodes are placed at different temperature zones. The inter-electrode temperature difference generates an electrical potential difference because of the temperature dependence of the $Fe(CN)_6^{3-}/Fe(CN)_6^{4-}$ redox potential.

When the cell is connected to an external electrical load, the thermally generated potential drives electrons in the external circuit so that an electrical current and power can be delivered. The continuous operation of a thermocell is achieved by the transport of the reaction product formed at one electrode to the other electrode, where it can then become a reactant. Natural convection based on the density gradient of the electrolyte can be a significant mode of transport in thermocells [20].

2.2. Fabrication of tubing-shaped, flexible thermocell

Aligned CNT sheets that are wrapped on a thin Pt wire were used as an electrode for improving thermocell performance. The most important advantage of nanocarbon electrodes is the characteristic high internal surface area, which can increase the number of available reaction sites per unit external area, resulting in increased power density [20]. The CNT sheets offer remarkable properties including high flexibility, thermal stability, high surface area (which can exceed 300 m^2/g) and ultra-low areal density (that can be below 3 $\mu g/cm^2$) [24,25]. To prepare the electrode, 1.0 cm width CNT sheet was continuously drawn from a sidewall of multi-walled CNT (MWCNT) forest using a dry-state spinning process (see Fig. 1(b)) and wrapped around a 200 μm diameter Pt wire using a connected rotating motor at 10 rpm. A percentile weight of CNT loading on the Pt wire can be easily controlled by the number of motor rotations. In order to find the optimal winding number of CNT sheets on a Pt wire, the winding number per unit Pt wire length was varied in the range 27–108 turns/cm with an interval of 27 turns/cm.

Fig. 1(c) presents the fabrication process of the thermocell used in this study. A highly flexible silicone tubing (Korea Ace Scientific) was used as a cell package with an inner and outer diameter of 3.0 and 4.5 mm, respectively. A 0.4 M potassium ferri/ferrocyanide (Sigma Aldrich) aqueous solution with a concentration close to saturation was used as the thermoelectric electrolyte. The electrolyte was prepared using deionized (DI) water and degassed prior to use by bath sonication. The freshly prepared electrolytes were incorporated immediately into the thermocell before commencing a series of measurements to avoid the effects of electrolyte degradation. The thermocell was assembled by inserting the CNT sheet electrodes in silicone tubing, followed by hot pressing both ends of the tubing at ~300 °C for 10 s. The electrolyte was injected into the cell through a syringe and the injection hole was sealed completely with epoxy.

2.3. Instruments and methods

Hot and cold temperatures were controlled by circulating water from a thermostatic bath (A&D Korea) with an accuracy of ±0.1 °C. The potential and current output from the cell was measured using a voltage–current meter (Keithley 2000 multimeter) to characterize the power output with respect to the external resistive loads. Scanning electron microscopy (SEM, Hitachi S-4700) was performed at an acceleration voltage of 10–15 keV.

3. Results and discussion

A tubing-shaped thermocell consisting of all flexible components, such as silicone tubing for packaging, CNT sheet electrodes and thermoelectric electrolytes, was fabricated to demonstrate the thermocell that is flexible enough to wrap onto the heat source of various shapes. The capability of power generation in the thermocell depends not only on the voltage, which is linearly proportional to the applied temperature difference, but also on the discharging currents. A large number of available reaction sites in the thermocell reaction result in increased power density. To prepare a thermocell electrode, two most important factors were considered in this study, which mainly determine the electrode performance: (1) the number of available reaction sites per unit external area, which is directly proportional to the reaction rate (*i.e.*, electric

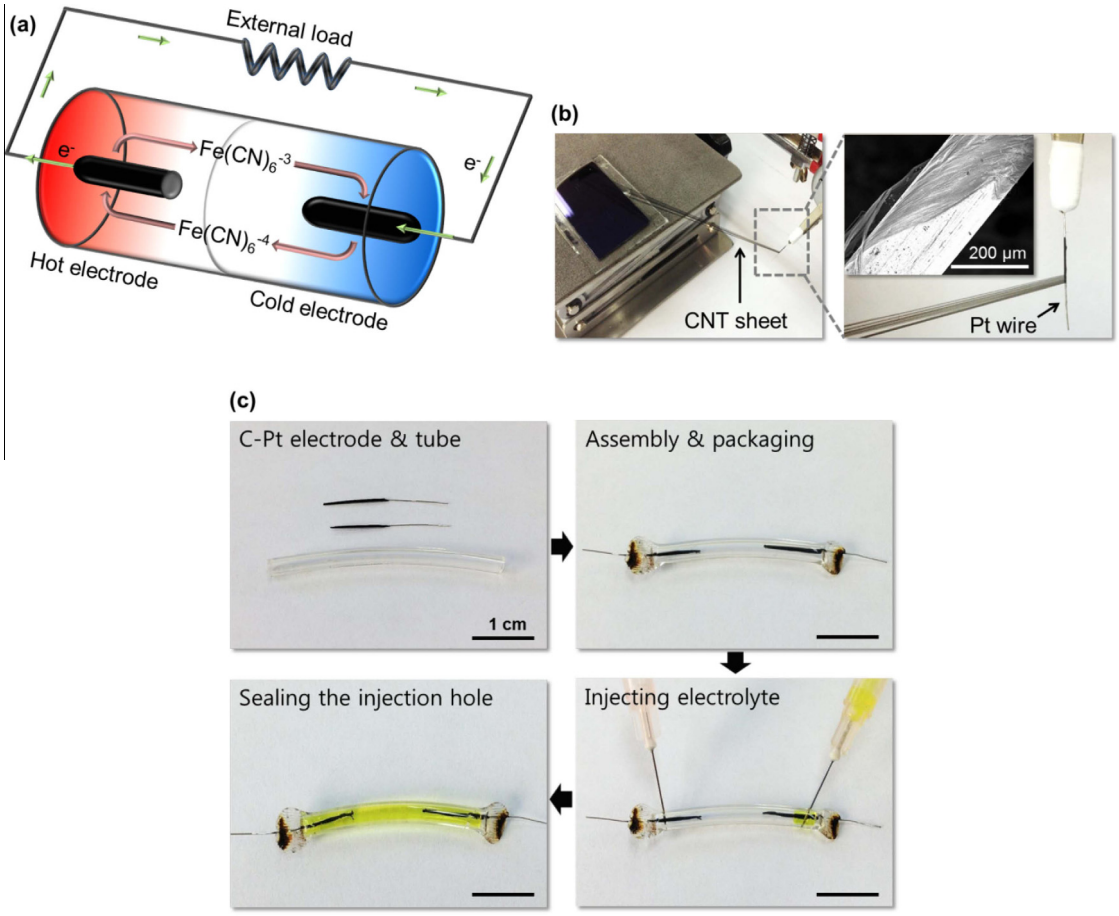

Fig. 1 – (a) Schematic diagram of thermocell operation. (b) Preparation of the CNT sheet electrode by dry-state spinning process. (c) Fabrication process of the tubing-shaped thermocell. (A color version of this figure can be viewed online.)

current); and (2) low electrical resistance for delivering the currents.

CNTs have been used widely in electrochemical applications owing to their high porosity and specific surface area, superior chemical stability, and excellent catalytic activity [26–28]. These properties of CNTs are also highly desirable for applications to thermocell electrodes. On the other hand, a one-dimensional, macroscopic form of CNTs, such CNT fibers and yarns, suffers from poor electrical conductivity along the length direction because of the contact resistance between the individual CNTs. A CNT sheet was wrapped onto a Pt wire to overcome the structural drawbacks in the electrical conductance of CNT fibers. The prepared electrode is a type of coaxial fiber with an inner Pt wire used as a current collector because of its good electrical conductivity, excellent catalytic activity and stability. CNT sheet layers wrapped onto platinum wire provide a high surface area for the thermocell reaction.

The electrode performance was examined by comparing the output powers from the thermocell using a bare Pt wire and CNT sheet wound electrodes. The inter-electrode temperature difference was maintained at 17.5 °C, the electrode spacing was set to 1 cm, and a 0.4 M ferri/ferrocyanide redox couple was used. To find the optimal winding number of CNT sheets on a Pt wire, the winding number per unit length was varied in the range 27–108 turns/cm with an interval of 27 turns/cm. The percentile weight of CNT loading on the Pt wire is calculated using the areal density of CNT sheet (~1.5 μg/cm^2). The effect of CNT sheet loading on the power generation is shown in Fig. 2(a). The measured output power was normalized to the cell area with an inner diameter of 3 mm. The result shows that the areal power density is maximized for 80 turns/cm of CNT sheet (corresponding to a CNT loading of 0.025 wt.%), providing a 1.6-fold higher power generation (from 8.76 to 14.2 μW/cm^2) compared to that of the Pt electrode. The discharge behavior was evaluated from the potential difference (E) versus current density (j) curve, as shown in Fig. 2(b).

Although identical open-circuit potentials were measured as ~25 mV by the temperature difference, the short-circuit current density (j_{sc}) increased from 1.3 to 2.4 mA/cm^2, which is responsible to the improved power generation by employing CNT sheets. This improvement is obviously due to the enlarged effective surface area of the CNT sheet by providing the number of available reaction sites. On the other hand, mass transport resistance, typically affected by ion accessibility into electrodes, might be increased when the CNT sheet loading increases [19,20,22]. It might drive sluggish ion diffusion within the electrode. Therefore, the power generation is maximized at an intermediate loading of CNT sheets (0.025 wt.%) as shown in Fig. 2(a).

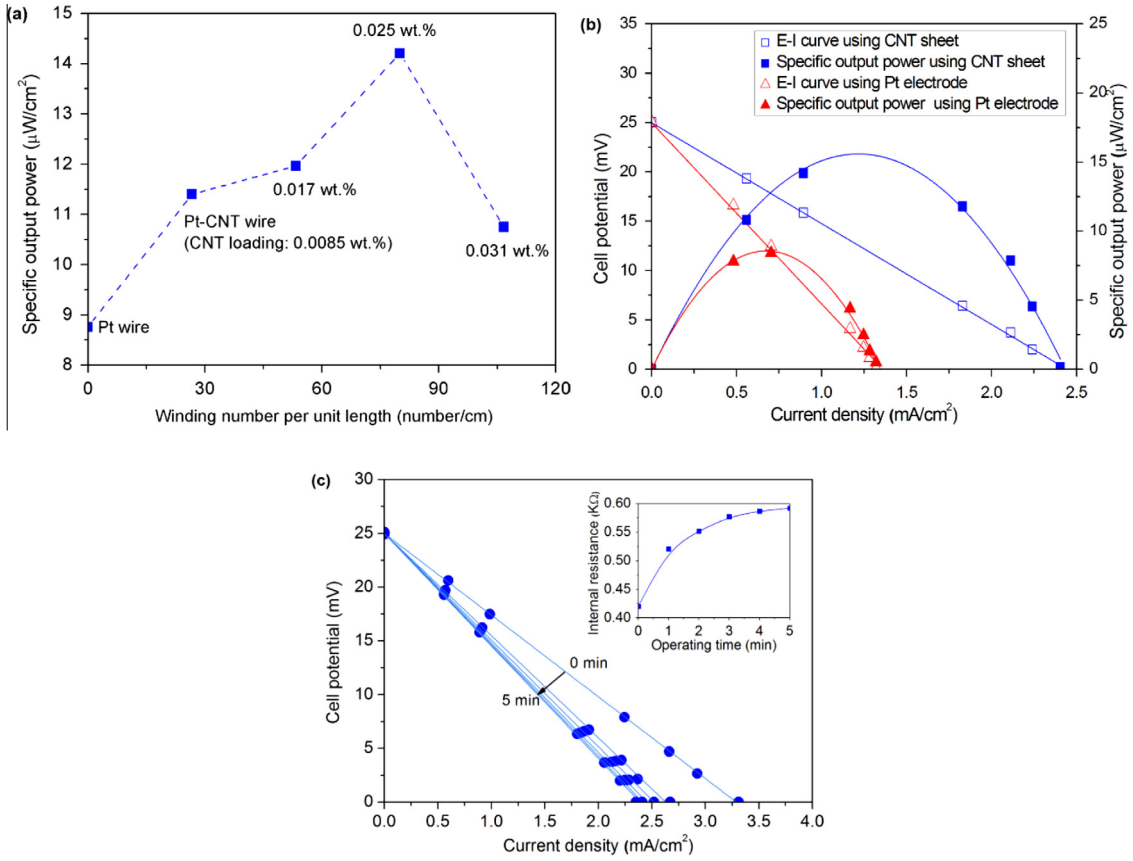

Fig. 2 – (a) Generation of output powers from the thermocell using a bare Pt wire and CNT sheet wound electrodes. (b) Comparison of the *E–j* curves and output powers from the thermocell using a bare Pt wire and CNT sheet wound electrodes. (c) Discharge behavior of the CNT sheet thermocell with increasing time from the start of operation; the insert shows the internal resistance of the thermocell with operating time. (A color version of this figure can be viewed online.)

For the continuous operation of a thermocell, the reaction product formed at one electrode should be transferred to the other electrode. For example, once the oxidation of ferrocyanide to ferricyanide begins at a hot electrode, the concentration of ferrocyanide ions at the electrode surface becomes smaller than that in the bulk solution. A significant concentration gradient occurs in the highly porous CNT sheet electrode. The CNT sheet electrode requires the development of an equilibrium concentration gradient in the electrode, which has not been observed for flat electrodes [20,23]. Therefore, the mass transport overpotential in the porous electrode results in the time dependent internal resistance of the thermocell [20]. Fig. 2(c) presents the discharge behavior of the CNT sheet thermocell as a function of time from the start of operation. The internal resistance of the CNT sheet thermocell (*i.e.*, the slope of *E–j* curve) increased from 0.42 to 0.59 kΩ and reached a steady state after 5 min operation (inset in Fig. 2(c)).

Based on the thermoelectric coefficient of the electrolyte, the open-circuit potential in a thermocell is determined basically by the inter-electrode temperature difference (ΔT). The temperature dependency on the thermocell performance was investigated by increasing the temperature at the hot electrode, while the temperature at the cold electrode was set to 10 °C. The other experimental conditions and measurement setups were the same as those used in Fig. 2. As the temperature difference increased from 14 to 21 °C with increasing 3.5 °C, the open-circuit potential and output current increased, as shown in Fig. 3(a), resulting in an increase in the maximum power generation from 7.63 for $\Delta T = 14$ °C to 23.4 μW/cm^2 for $\Delta T = 21$ °C.

It is evident that the open-circuit potential is linearly proportional to the current density from Fig. 3(a). The maximum output power is expected to be quadratically proportional to the temperature difference. However, the measured output power was increased beyond the expected ΔT^2 dependence. The enhanced power generation might be due to the lower internal resistance of the thermocell. Fig. 3(b) shows that the internal resistance of the thermocell decreases by 28% (from 0.78 to 0.56 kΩ) with increasing average temperature between the two electrodes (*i.e.*, the operating temperature). Increasing the operating temperature will increase the redox reactivity at the electrodes, as well as increase the ionic conductivity of the electrolyte and diffusion processes within the porous CNT sheet electrodes. Changing the temperature has an exponential effect on the exchange current density, as described by the Butler–Volmer equation [29]. Moreover, the charge-transfer, ohmic and mass transport overpotentials can be reduced simultaneously by increasing the operating temperature.

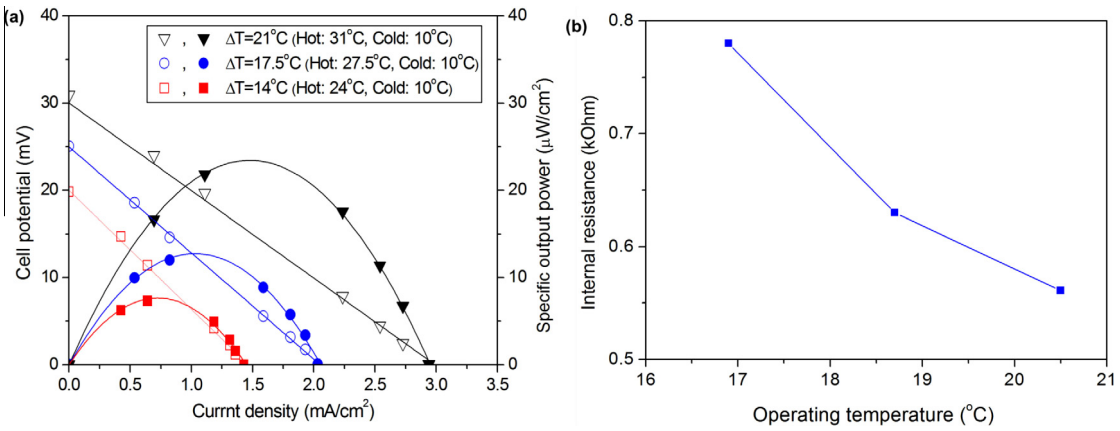

Fig. 3 – (a) Temperature dependency on the thermocell performance by increasing the temperature at the hot electrode, while the temperature at the cold electrode was set to 10 °C. (b) Internal resistance of the thermocell with a variation of the operation temperature. (A color version of this figure can be viewed online.)

The series connection of two identical cells was examined to demonstrate the voltage and power scaling, as shown in Fig. 4(a). The thermocells in a series connection generated a voltage of approximately 50 mV, which is equal to the sum of the open circuit voltages of the individual cell with an inter-electrode temperature of 17.5 °C. The maximum output power of the serially connected cells was measured to be ~26 μW/cm^2, which is approximately equal to the sum of the maximum output powers of the two cells when they are operated individually. The total voltage of the serially connected cells will be doubled but the internal resistance of the cells is also doubled for the system, with the relationship, $P = V^2/R$, which amounts to twice the power of a single cell.

To demonstrate the flexibility of the present thermocell, the wire-shaped thermocell was wrapped around two stainless steel cups, as shown in the inset in Fig. 4(b). When cold water was poured into one cup, the cell potential increased due to the temperature difference between the two cups, and stabilized after 3 min. The output voltage was increased further by pouring hot water into the other cup, as shown in the figure. Such a scheme of wiring a thermoelectric harvester can be achieved because of the flexibility of the present cell based on liquid thermoelectrics, whereas conventional solid thermoelectric materials are difficult to deploy.

4. Conclusions

A tubing-shaped, flexible thermocell was fabricated using CNT sheet electrodes. A highly porous CNT sheet that is wrapped on a thin platinum (Pt) wire was used as an electrode for the redox reaction. The electrode performance was examined by comparing the output power from the thermocell using a bare Pt wire and CNT sheet wound electrodes. After employing the CNT sheet electrode, the higher output power could be delivered from 8.5 to 15.6 μW and the short-circuit current density was increased ~1.8-fold compared to that of the Pt wire electrode. The internal resistance of the thermocell was decreased by 28% (from 0.78 to 0.56 kΩ) with increasing operating temperature. The open-circuit potential and output current increased as the temperature difference was

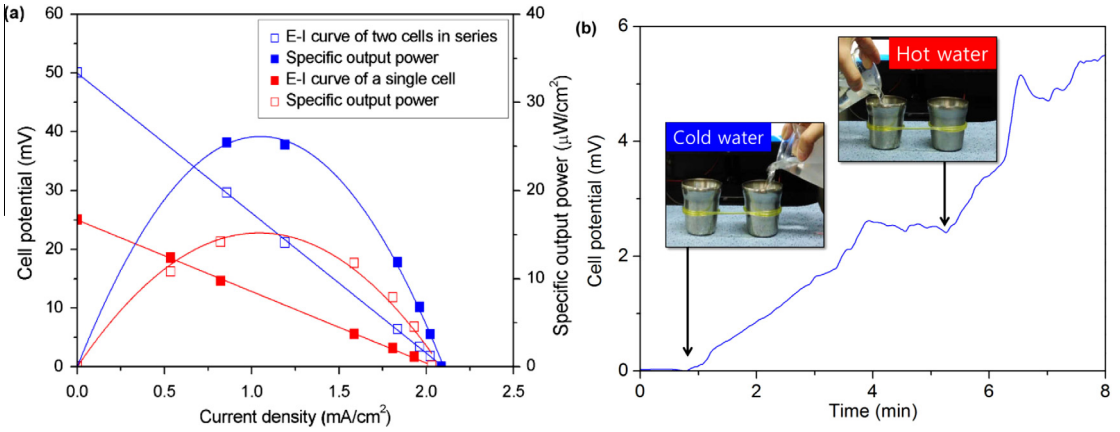

Fig. 4 – (a) *E–I* curves and the specific output power of a single cell and serially connected two cells. (b) Demonstration of the present thermocell wrapped onto two stainless steel cups at different temperature sources. (A color version of this figure can be viewed online.)

increased from 14 to 21 °C with an increment of 3.5 °C, resulting in an increase in the maximum power generation from 7.63 for $\Delta T = 14$ °C to 23.4 $\mu W/cm^2$ for $\Delta T = 21$ °C. Compared to solid thermoelectric materials, the present thermocell showed a range of advantages, such as simple and low cost fabrication and high flexibility.

Acknowledgements

This research was supported in Korea by the National Research Foundation of Korea (Grants 2014R1A1A4A01008768), and the Civil & Military Technology Cooperation Program through the National Research Foundation of Korea (NRF) funded by the Ministry of Science, ICT & Future Planning (No. 2013M3C1A9055407).

REFERENCES

[1] Hicks L, Dresselhaus M. Effect of quantum-well structures on the thermoelectric figure of merit. Phys Rev B 1993;47(19):12727.
[2] Hicks L, Dresselhaus M. Thermoelectric figure of merit of a one-dimensional conductor. Phys Rev B 1993;47(24):16631.
[3] Hochbaum AI, Chen R, Delgado RD, Liang W, Garnett EC, Najarian M, et al. Enhanced thermoelectric performance of rough silicon nanowires. Nature 2008;451(7175):163–7.
[4] Mahan G, Sales B, Sharp J. Thermoelectric materials: new approaches to an old problem. Phys Today 2008;50(3):42–7.
[5] Poudel B, Hao Q, Ma Y, Lan Y, Minnich A, Yu B, et al. High-thermoelectric performance of nanostructured bismuth antimony telluride bulk alloys. Science 2008;320(5876):634–8.
[6] Snyder GJ, Toberer ES. Complex thermoelectric materials. Nat Mater 2008;7(2):105–14.
[7] Terasaki I, Sasago Y, Uchinokura K. Large thermoelectric power in NaCo 2 O 4 single crystals. Phys Rev B 1997;56(20):R12685.
[8] Venkatasubramanian R, Siivola E, Colpitts T, O'quinn B. Thin-film thermoelectric devices with high room-temperature figures of merit. Nature 2001;413(6856):597–602.
[9] Bell LE. Cooling, heating, generating power, and recovering waste heat with thermoelectric systems. Science 2008;321(5895):1457–61.
[10] Chen G, Dresselhaus M, Dresselhaus G, Fleurial J-P, Caillat T. Recent developments in thermoelectric materials. Int Mater Rev 2003;48(1):45–66.
[11] DiSalvo FJ. Thermoelectric cooling and power generation. Science 1999;285(5428):703–6.
[12] Dughaish Z. Lead telluride as a thermoelectric material for thermoelectric power generation. Physica B 2002;322(1):205–23.
[13] Gunawan A, Lin C-H, Buttry DA, Mujica V, Taylor RA, Prasher RS, et al. Liquid thermoelectrics: review of recent and limited new data of thermogalvanic cell experiments. Nanoscale Microscale Thermophys Eng 2013;17(4):304–23.
[14] Riffat SB, Ma X. Thermoelectrics: a review of present and potential applications. Appl Therm Eng 2003;23(8):913–35.
[15] Abraham TJ, MacFarlane DR, Pringle JM. Seebeck coefficients in ionic liquids–prospects for thermo-electrochemical cells. Chem Commun 2011;47(22):6260–2.
[16] Abraham TJ, MacFarlane DR, Pringle JM. High Seebeck coefficient redox ionic liquid electrolytes for thermal energy harvesting. Energy Environ Sci 2013;6(9):2639–45.
[17] Bonetti M, Nakamae S, Roger M, Guenoun P. Huge Seebeck coefficients in nonaqueous electrolytes. J Chem Phys 2011;134(11):114513.
[18] Hu R, Cola BA, Haram N, Barisci JN, Lee S, Stoughton S, et al. Harvesting waste thermal energy using a carbon-nanotube-based thermo-electrochemical cell. Nano Lett 2010;10(3):838–46.
[19] Im H, Moon HG, Lee JS, Chung IY, Kang TJ, Kim YH. Flexible thermocells for utilization of body heat. Nano Res. 2014;7(4):1–10.
[20] Kang TJ, Fang S, Kozlov ME, Haines CS, Li N, Kim YH, et al. Electrical power from nanotube and graphene electrochemical thermal energy harvesters. Adv Funct Mater 2012;22(3):477–89.
[21] Salazar PF, Kumar S, Cola BA. Nitrogen-and boron-doped carbon nanotube electrodes in a thermo-electrochemical cell. J Electrochem Soc 2012;159(5):B483–8.
[22] Salazar PF, Kumar S, Cola BA. Design and optimization of thermo-electrochemical cells. J Appl Electrochem 2014;44(2):325–36.
[23] Quickenden T, Mua Y. A review of power generation in aqueous thermogalvanic cells. J Electrochem Soc 1995;142(11):3985–94.
[24] Aliev AE, Oh J, Kozlov ME, Kuznetsov AA, Fang S, Fonseca AF, et al. Giant-stroke, superelastic carbon nanotube aerogel muscles. Science 2009;323(5921):1575–8.
[25] Zhang M, Fang S, Zakhidov AA, Lee SB, Aliev AE, Williams CD, et al. Strong, transparent, multifunctional, carbon nanotube sheets. Science 2005;309(5738):1215–9.
[26] Gong K, Yan Y, Zhang M, Su L, Xiong S, Mao L. Electrochemistry and electroanalytical applications of carbon nanotubes: a review. Anal Sci 2005;21(12):1383–93.
[27] Gooding JJ. Nanostructuring electrodes with carbon nanotubes: a review on electrochemistry and applications for sensing. Electrochim Acta 2005;50(15):3049–60.
[28] Luo H, Shi Z, Li N, Gu Z, Zhuang Q. Investigation of the electrochemical and electrocatalytic behavior of single-wall carbon nanotube film on a glassy carbon electrode. Anal Chem 2001;73(5):915–20.
[29] O'Hayre RP, Cha S-W, Colella W, Prinz FB. Fuel cell fundamentals; 2006.